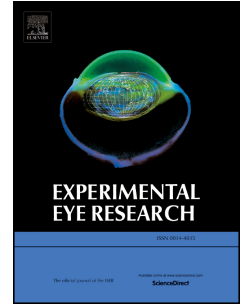# Accepted Manuscript

Imaging of macrophage dynamics with optical coherence tomography in anterior ischemic optic neuropathy

Despina Kokona, Nathanael U. Häner, Andreas Ebneter, Martin S. Zinkernagel

Please cite this article as: Kokona, D., Häner, N.U., Ebneter, A., Zinkernagel, M.S., Imaging of macrophage dynamics with optical coherence tomography in anterior ischemic optic neuropathy, *Experimental Eye Research* (2016), doi: 10.1016/j.exer.2016.11.020.

Imaging of macrophage dynamics with optical coherence tomography in anterior ischemic optic neuropathy

Despina Kokona PhD[1], Nathanael U Häner[1], Andreas Ebneter MD PhD[1,2], and Martin S Zinkernagel MD PhD[1,2]

1 Department of Ophthalmology, Inselspital, Bern University Hospital, and University of Bern, Bern, Switzerland

2 Department of Clinical Research, Inselspital, Bern University Hospital, and University of Bern, Bern, Switzerland

The authors declare that they have no conflicts of interest

Corresponding author:

Martin Zinkernagel, MD, PhD

Dept. Ophthalmology, Inselspital, Universität Bern

CH-3010 Bern, Tel: +41 (0) 31 632 95 65, FAX:

martin.zinkernagel@insel.ch

Abbreviations:

A-AION, arteritic anterior ischemic optic neuropathy; AMD, age-related macular degeneration; CNS, central nervous system; CNV, choroid neovascularisation; CX3CR1, C-X3-C motif chemokine receptor 1; DME, diabetic macular edema; eAION, experimental anterior ischemic optic neuropathy; eLiON, experimental laser-induced optic neuropathy; FACS, fluorescence-activated flow cytometry; GCL, ganglion cell layer; INL, inner nuclear layer; IPL, inner plexiform layer; NA-AION, nonarteritic anterior ischemic optic neuropathy; OCT, optical coherence tomography; ON, optic nerve; ONH, optic nerve head; ONL, outer nuclear layer; OPL, outer plexiform layer; RVO, retinal vein occlusion; SD-OCT, spectral-domain optical coherence tomography; WT, wild type

ABSTRACT

Anterior ischemic optic neuropathy (AION) is a relatively common cause of visual loss and results from hypoperfusion of the small arteries of the anterior portion of the optic nerve. AION is the leading cause of sudden optic nerve related vision loss with approximately 10 cases per 100'000 in the population over 50 years. To date there is no established treatment for AION and therefore a better understanding of the events occurring at the level of the optic nerve head (ONH) would be important to design future therapeutic strategies. The optical properties of the eye allow the imaging of the optic nerve in vivo, which is a part of the CNS, during ischemia. Experimentally laser induced optic neuropathy (eLiON) displays similar anatomical features as anterior ischemic optic neuropathy in humans. After laser induced optic neuropathy we show that hyperreflective dots in optical coherence tomography correspond to mononuclear cells in histology. Using fluorescence-activated flow cytometry (FACS) we found these cells to peak one week after eLiON. These observations were translated to OCT findings in patients with AION, where similar dynamics of hyperreflective dots at the ONH were identified. Our data suggests that activated macrophages can be identified as hyperreflective dots in OCT.

1. INTRODUCTION

Our sense of sight depends on an intact optic nerve (ON) which relays the visual information from the retina to the brain. The ON is part of the central nervous system (CNS) and is composed of myelinated retinal ganglion cell axons and supporting glial cells. Anterior ischemic optic neuropathy (AION) results from hypoperfusion or nonperfusion of the anterior part of the ON and is considered to be the equivalent of a white matter stroke (Hayreh, 2014; Bernstein et al., 2003). AION is the most common cause for sudden optic nerve related vision loss in patients over 50 and can be divided into a nonarteritic form (NA-AION) and an arteritic form (A-AION) (Hayreh, 1974) . NA-AION causes about 85% of sudden optic nerve-related vision loss and typically affects individuals over 55 years of age. Although the exact pathophysiology of NA-AION is complex and not fully understood, numerous risk factors have been identified including vascular disorders such as systemic hypertension (Hayreh et al., 1994; Guyer et al., 1985; Salomon et al., 1999), diabetes mellitus (Lee et al., 2011) and smoking (Chung et al., 1994). A-AION is less common and usually affects persons over the age of 70 and is the most common ophthalmic manifestation of giant cell arteritis. The clinical course of both forms of AION is characterized by a sudden monocular loss of vision with edema of the optic disc resulting from axonal ischemia and localized infarction of the ON. Similar to CNS stroke where ischemia has been shown to elicit a profound inflammatory response mediated by proinflammatory cytokines and recruitment of leukocytes (Low et al., 2014), inflammation has been reported to play a role in AION as well (Goldenberg-Cohen et al., 2004; Salgado et al., 2011). Because these observations are based on histology, there is scarce information on *in vivo* dynamics of leukocyte infiltrate after white matter ischemia.

Because of its unprecedented resolution, spectral-domain optical coherence tomography (SD-OCT) has the potential to image leukocytes within the ON and the surrounding retinal tissue, with a resolution in the range of 5 µm to 7 µm, which exceeds the 10-25 µm measured for macrophages (Douglas and Tuluc, 2012).

So called hyperreflective dots have recently been described in SD-OCT in diabetic macular edema and in intraocular inflammatory disorders (Vaz-Pereira et al., 2015; Saito et al., 2013) and have been attributed to inflammatory cells, although this has not been confirmed by histology so far. In this study we show that hyperreflective dots seen in SD-OCT may correspond to macrophages in a mouse model of experimentally laser-induced optic neuropathy (eLiON) and that there is a characteristic time course of macrophage influx into the ON and the surrounding retina in the mouse which corresponds to the appearance of hyperreflective dots in the OCT of patients with AION.

2. METHODS

2.1 Animal experiments

Male and female BALB/c wild-type (WT) mice were obtained from Charles River Laboratories (Sulzfeld, Germany). Male and female $Cx_3cr1^{+/gfp}$ transgenic mice on a BALB/c background (more than 6 backcrosses to generate homozygous mice) were kindly provided by Prof. Steffen Jung (Weizmann Institute of Science, Rehovot, Israel) and homozygous mice were bred at the Central Animal Facility of the University of Bern (Murtenstrasse 31, Bern, Switzerland). CX3CR1^{gfp} transgenic mice were generated by targeted replacement of the fractalkine receptor CX3CR1 gene with the cDNA encoding GFP (Jung et al., 2000). Thus, GFP is specifically expressed in microglia/macrophages of CX3CR1^{gfp} mice.

Male/female BALB/c AnNCrl (6-8 weeks old, Charles River Laboratories, Sulzfeld, Germany) and CX3CR1$^{gfp/gfp}$ BALB/c mice (6 weeks old) were used in the present study. The animals were housed under pathogen free, temperature and humidity-controlled conditions in individually ventilated cages with an alternating 12-hour light/12-hour dark cycle. Food and water were provided ad libitum. For the eLiON induction and the SD-OCT studies the mice were anesthetized by intraperitoneal injection of ketamine (90 mg/kg, Ketalar, Orion Pharma AG, Zug, Zurich, Switzerland) and medetomidine hydrochloride (1.5 mg/kg, Domitor; Orion Pharma AG, Zug, Zurich, Switzerland). Atipamezol (Antisedan 5 mg/mL, Orion Pharma AG, Zug, Zurich, Switzerland) was used to antagonize medetomidine hydrochloride at the end of the intervention. At the end of the experiment, mice were euthanized with carbon dioxide (CO_2) inhalation using 100% CO_2 with a fill rate of about 30% of the chamber volume per minute.

2.2 Generation of Bone Marrow Chimeras

To identify the origin of microglia/macrophages in the retina we used CX3CR1$^{gfp/gfp}$ BALB/c mice which express GFP under the promoter of CX3CR1. Recipient mice received 12-Gy γ-ray full body irradiation in two doses of 14 hours apart (6-Gy per dose). Donor mice were euthanatized, and femurs and tibia were harvested. Bone marrow was flushed out from bones with CSM buffer (2% FBS, 1% antibiotics, 0.01M HEPES in HBSS), and single cell suspensions were generated. The cells were filtered through a 70 μm mesh filter and centrifuged at 300 rpm for 5 min at 4°C. The pellet was re-suspended in 2% FBS in DMEM medium (Thermofisher scientific, Waltham, Massachusetts, USA) and trypan blue was used for the counting of the live cells. Recipient mice received 1 to 2×10^6 bone marrow cells intravenously in a maximum of 3 hours after the second dose of irradiation. Bone marrow chimera mice were left to recover for two weeks before any further intervention. During this

period mice received water supplied with antibiotics (0.8mg/ml sulfamethoxazol and 0.16 mg/ml trimethoprim).

2.3 Experimental laser-induced optic neuropathy (eLiON)

Experimental LiON was induced by a 532 nm laser photocoagulation (Visulas 532s, Carl Zeiss Meditec AG). A spot size of 500 μm with an energy level of 200 mW and 2.5s duration were used to directly target the optic nerve. Prior to the laser application rose bengal (40 mg/kg, Sigma-Aldrich) was injected intravenously to increase the laser uptake. Pupils were dilated with tropicamide 0,5%/phenylephrine 2,5% eye drops (Hospital Pharmacy, Inselspital, Bern, Switzerland).

2.4 Tissue preparation and immunohistochemical studies

At selected time points, mice were euthanized and their eyes were removed and fixed in 4% parafolmaldehyde solution (PFA, pH 7.4) for 24 hours. Eyes were processed for routine paraffin embedding and slices of 5 μm were collected with a microtome (Leica, Biosystems, Muttenz, Switzerland) from the central retina containing the optic nerve head. Single staining with a rabbit polyclonal antibody against Iba-1 (1:5000, 016-20001, WAKO chemicals, Richmond, VA, USA) was performed in control and eAION BALB/c mice using a biotinylated anti-rabbit IgG (H&L) antibody (Vector Laboratories, BA-100, Burlingame, CA, USA) followed by incubation in a streptavidin Alexa Fluor 488 conjugate antibody (Thermo Fisher Scientific, S32354, Waltham, MA, USA). To investigate the infiltration of microglia cells into the retina during the course of AION, co-localization studies were performed in chimera mice using a chicken polyclonal antibody against GFP (1:100, ab13970, Abcam, Cambridge, UK) and a rabbit polyclonal antibody against Iba-1 (1:5000, 016-20001, WAKO chemicals, Richmond, VA, USA). Briefly, the sections were routinely de-paraffinized and

peroxidase activity was blocked by incubation in 0.5% H_2O_2 in methanol. The retrieval of the antigen epitopes was achieved by incubation in citrate buffer (10 mM, pH 6.0, 95 °C, 10 min). The secondary antibodies pre-absorbed goat polyclonal to chicken IgY H&L (FITCH) (1:1000, ab7114, Abcam, Cambridge, UK) and goat anti-rabbit IgG (H+L), Alexa Fluor 594 conjugate (1:1000, A27016, Thermofisher scientific, Waltham, Massachusetts, USA) were used for the detection of GFP and Iba-1, respectively. Slides were mounted in mounting medium with DAPI (Vector Laboratories, Burlingame, CA, USA), cover slipped and observed in the microscope.

2.5 Histological staining

For the evaluation of morphological changes, retinal sections from experimental mice were histologically examined, using a standard hematoxylin-eosin staining protocol 7 days after the eLION induction. Briefly, the sections were routinely de-paraffinized in xylol, rehydrated and consecutively stained with hematoxylin and eosin. Dehydration of the sections was achieved with ethanol. Finally, the sections were mounted with Eukitt (O. Kindler GmbH & Co, Freiburg, Germany).

2.6 Microscopy

Light and optical microscopy images were taken with an epifluorescence microscope (Olympus BX60 microscope; Olympus, Tokyo, Japan). Adjustments of light and contrast were achieved with the use of the commercial software Photoshop ver. 7.0 (Adobe Systems, San Jose, CA) and the figures were finalized in CorelDraw (Corel Corporation of Ottawa, Canada).

2.7 Fluorescence-Activated Flow Cytometry - FACS analysis

Retinas were processed for FACS analysis 3, 7 and 14 days after eLiON induction. Briefly, the retinas were isolated and dissociated in 0.4 Wünsch Liberase TM Grade (Roche, Basel, Switzerland) in DPBS/0.01% DNAse I (Roche, Basel, Switzerland) at 37 ℃ for 30 min. Single cell suspensions were obtained and re-suspended in 500μl DPBS/0.01% DNAse. 1μl of DAPI (Thermo Fisher Scientific, Waltham, MA, USA) was added in each sample and the samples were incubated for 30sec at RT for the staining of dead cells. The samples were washed in DPBS/0.01% DNAse and re-suspended in 200μl of FACS buffer (100mM EDTA, 20% FBS, 0.5% Na-Azide, in DPBS/DNAse 0.01%) for antibody staining. Macrophages were identified using fluorescent-labelled antibodies against CD45 (30-F11, #103116, 1:100), F4/80 (BM8, #123110, 1:60), CD11b (M1/70, #101212, 1:100), MHC-II (major histocompatibility complex class-II, AF6-120.1, #116422, 1:100) and CD68 (FA-11, #137010, 1:100). Samples were incubated for 20min in the antibody pool, washed again and re-suspended in 800μl of FACS buffer. Samples were analyzed in a LSR II Cytometer System and the BD FACSDIVA™ software (BD Biosciences, Allschwil, Switzerland). Flowjo Single Cell Analysis Software V10 was used for the analysis of the FACS data (TreeStar, Ashland, OR). All antibodies were purchased from Biolegend (San Diego, California, USA).

2.8 Patient selection

This study was based on retrospective analysis of data from patients of the outpatient clinic of the Department of Ophthalmology at the University Hospital Bern, Switzerland back to the year 2007. Patients were selected from the database of back-up reports. Patients with a history of age-related macular degeneration (AMD), choroid neovascularisation (CNV), glaucoma and all cases before the year 2007 (no OCT have been made before 2007) were excluded. Of the remaining 129 patients, 68 had been examined by OCT at least once. In 33 cases, OCT had been performed in the acute phase of AION with follow up OCTs. Of these 33 patients 10 had A-AION and 23 had NA-AION.

2.9 Spectral Domain Optical Coherence Tomography – SD-OCT

Mice: OCT images of mice were taken with a SD- OCT (Heidelberg Engineering GmbH, Heidelberg, Germany) that was adapted for mouse imaging. A 78D ophthalmic slit lamp lens (Volk Optical Inc., Ohio, USA) was adjusted on the standard 30° Heidelberg Spectralis lens and a contact lens (Quantum I, Bausch + Lomb Inc., Rochester, NY) was placed on the mouse eye. OCT images of patients were acquired with a SD- OCT (Heidelberg Engineering GmbH, Heidelberg, Germany) with a scan around the optic nerve head.

Ambient light was reduced to nearly zero lux for noise reduction. The images were taken in 'grid mode' and 'cylindrical mode' at high resolution (1008 x 596 pixels). Infrared images were obtained at a resolution of 1'536 x 1'536 pixels.

2.10   Quantification studies

Hyperreflective dots were counted manually on cylindrical OCTs of human patients obtained with the Heidelberg software. Cylindrical OCTs were acquired in a diameter of 3.4 ± 0.04 mm (mean $\pm$ S.E.M.) around the optic nerve head. Quantification of the OCT data was performed at different time points after initial symptoms. Time after initial symptoms was defined as the time after onset of the patient's initial symptoms.

Mouse retinal thickness was quantified using the Heidelberg software after manual correction of the base membrane and inner limiting membrane. Vertical scans from the centre of the optic nerve were used for the quantification.

2.11 Statistics

For the statistical analysis the GraphPad Prism 5.0 software was used (GraphPad Software, Inc, San Diego, CA, USA). Statistically significant differences of the OCT quantification data were determined using ordinary one way ANOVA followed by Tukey`s

post-hoc tests. One way ANOVA followed by Tukey post hoc analysis tests was used for the determination of statistically significant differences of the FACS data. Two way ANOVA was used for the statistical analysis of retinal thickness measurements. P values less than 0.05 were considered statistically significant. All data are expressed as mean ± S.E.M.

2.12 Study approval

All animal procedures were conducted in accordance with the ARVO Statement for the Use of Animals in Ophthalmic and Vision Research and was approved by the local Animal Ethics Committee (Veterinärdienst des Kantons Bern: BE 38/13).

The human study followed the tenets of the Declaration of Helsinki, and Ethics Committee approval had been obtained (KEK-Nr. 370/14).

3. RESULTS

3.1 Macrophage accumulation in the optic nerve and surrounding retina after eLiON

Optical coherence tomography of the optic nerve head in naïve animals showed a well-defined optic nerve head with intact layers of the surrounding retinal layers. Furthermore hyperreflective dots were absent in the optic nerve head and the vitreous (Figure 1A,C). Three days after induction of eLiON, there was marked swelling of the optic nerve head with hyperreflective dots appearing within the optic nerve head and the vitreous (Figure 1B) and mononuclear cells within the optic nerve head and the vitreous in H&E stains (Figure 1D).

To localize and to identify blood-borne macrophages in the optic nerve head, we used bone marrow chimera mice that were lethally irradiated and transplanted with GFP-expressing bone marrow cells. Co-localization within the ischemic area revealed that these GFP$^+$ cells expressed Iba-1 and confirmed that they derived from the circulating bone marrow derived

myeloid population and not activated microglia from the host's resident ON population. Iba-1 is a microglia/macrophage-specific calcium binding protein that is expressed by macrophages and central nervous system microglial cells (Ahmed et al., 2007). In control mice, GFP expression was absent on Iba-1 positive cells (Figure 1F) and these cells were less abundant compared to eLiON mice (Figure 1J). Moreover, microglial Iba-1^{+} cells had a ramified phenotype characterized by a small soma and thin cell processes, typical for resting microglia (Figure 1G) (Wilms et al., 1997). In contrast, GFP[+]Iba1^{+} cells in eLiON mice displayed a more phagocytic-like phenotype with round cytosol and retracted processes (Figure 1 H&I), corresponding to activated macrophages. Analysis of conventional hematoxylin and eosin histology confirmed swelling of the optic nerve head (asterisk in Figure 1D) with dilatation of optic nerve head vessels (Figure 1D).   Optic nerve injury was also present in eLiON eyes accompanied by formation of retinal folds in the peripapillary area (Figure 1D).

3.2 Quantification and time course of macrophage accumulation in the ON and the surrounding retina in eLiON

Quantification of retinal thickness in mouse retinas revealed statistically significant swelling of the ON and the surrounding retina in the eLiON mice 3 days after the laser application (Figure 2A).   For quantification of macrophage populations in eLiON, fluorescence-activated flow cytometry (FACS) was performed in eLiON and controls at different time points after the laser application. The number of CD45+CD11b+F4/80+ cells, representing macrophages, increased significantly 7 days after eLiON (Figure 2C, top graph, ***$p < 0.001$ compared to control). Thereafter macrophage numbers decreased but were still elevated compared to controls (Figure 2C, top graph, **$p < 0.01$ compared to control). In order to assess whether these macrophages were activated, we assessed up regulation of major histocompatibility complex class 2 (MHC-II) and CD68. The numbers of CD68^{+}MHC-II^{+}

cells were significantly elevated 7 days after the laser application confirming that these macrophages were activated, while these numbers rapidly decreased and reached similar levels as the controls at day 14 (Figure 2C, bottom graph, ***p<0.001 compared to control).

3.3 Correlation between SD-OCT findings in eLiON and AION in humans

Thirty three patients with AION were included and demographic data is summarized in table 1. Ten patients had A-AION and 23 patients had NA-AION. The indication for OCT imaging was made in the clinical routine to analyze peripapillary nerve fibre thickness (Figure 2E). This resulted in a heterogenous sampling rate and follow up time. The A-AION patient group included 4 males and 6 females with a mean age of 77± 6.9 years. Giant cell arteritis was verified in all 10 patients by a positive biopsy-result of the temporal artery. The NA-AION patient group included 13 males and 10 females with a mean age of 67± 13.0 years. Figure 2E shows representative images obtained from cross section (upper panels) and cylindrical OCTs (bottom panels) in humans one week after initial symptoms. Both in mice (Figure 2B) and humans a marked swelling of the nerve fibre layer of the optic nerve head can be seen. Furthermore, hyperreflective dots can be observed in both eLiON and AION eyes, especially in the optic nerve head and the surrounding retina and within the vitreous.

3.4 Quantification and time course of inflammatory cells in SD-OCT in patients with AION

Peripapillary SD-OCT scans were performed in human patients at various time points after initial symptoms of AION. Hyperreflective dots in the retina as well as in the vitreous were observed, similar to the hyperreflective dots observed in eLiON mice. Manual counts of the number of hyperreflective dots in the retina (peripapillary area) peaked 2 weeks after initial reported symptoms and declined thereafter (Figure 2F bottom, p<0.01, ordinary one was ANOVA). Tukey`s post-hoc analysis revealed statistical significant reduction of

hyperreflective dot counts between 2 weeks and 15-70 weeks after initial symptoms **$p<0.01$). On the other hand, hyperreflective dots were less abundant in the vitreous (Figure 2F, top). No significant differences were observed in the number of hyperreflective dots between A-AION and NA-AION patients neither in the retina nor in the vitreous (data not shown), however as all A-AION patient received high dose corticosteroid treatment, this data needs to be interpreted with caution. Quantification of hyperreflective dots in different retinal layers revealed elevated numbers in the outer plexiform layer (OPL) ($p<0.01$, ordinary One way ANOVA) and the outer nuclear layer ($p<0.05$, ordinary One way ANOVA) (ONL) which peaked at 2 weeka after initial symptoms and decreased over time (Figure 3A-E). Statistically significant differences were observed between different time points in the INL (Figure 3E; week 2 vs week 15-70, *$p<0.05$; ordinary One way ANOVA followed by Tukey`s post-hoc analysis) and the OPL (Figure 3E; week 2 vs week 15-70, *$p<0.05$; ordinary One way ANOVA followed by Tukey`s post-hoc analysis). No statistically significant difference was observed in the inner retinal layers such as the nerve fibre layer and the ganglion cell layer (Figure 3E).

4. DISCUSSION

It is well accepted that acute ischemia of the anterior part of the optic nerve head is the cause of AION which is followed by retinal ganglion cell axon degeneration and apoptotic cell death of the ganglion cells (Levin and Louhab, 1996). It has been recently suggested that similar to inflammation following CNS stroke, inflammatory processes may play a role in the course of AION as well (Zhang et al., 2009; Goldenberg-Cohen et al., 2004; Salgado et al., 2011). However, the majority of these observations are based on histological findings, and few *in vivo* data is available regarding the dynamics of leukocyte infiltration after white matter ischemia in general.

In the present study a murine model of laser-induced optic neuropathy (eLiON), characterized by optic nerve injury and optic nerve swelling, in combination with *in vivo* imaging using optical coherence tomography was used for the investigation of the dynamics of microglia/macrophages during the disease. The co-localization of microglia marker Iba-1 with GFP - expressed on circulating myeloid derived cells of CX3CR1$^{gfp/gfp}$ mice - showed that blood derived circulating macrophages migrate into the optic nerve and surrounding retina during the early stages of eLiON. However, despite the fact that all GFP positive cells were co-localized with Iba-1, this was not a "vice versa phenomenon", suggesting that the activated macrophages population during the course of eLiON correspond both to the activation of resident microglia and to the recruitment of circulating macrophages. Indeed, activation of microglia has been reported using histology in rodent models of optic nerve injury (Garcia-Valenzuela and Sharma, 1999; Zhang and Tso, 2003; Thanos, 1992) and infiltration of macrophages has been observed in the optic nerve of rats and primates subjected to eAION (Slater et al., 2013; Salgado et al., 2011). Resident microglia - present in the retina and the brain in a resting stage- are activated under infectious and inflammatory

conditions and contribute to the maintenance of tissue homeostasis by removing cellular debris (Langmann, 2007).

SD-OCT was used as a non-invasive technique for the investigation of retinal alterations in eLiON mice. OCT scans revealed the appearance of hyperreflective dots in the retina and vitreous of eLiON-subjected mice 3 days after the induction of the disease. Interestingly, a similar morphology and time course of hyperreflective dots was identifiable in humans diagnosed with AION during the acute phase of the disease, namely 1-2 weeks after the initial symptoms of visual deficits. This difference may be explained by the fact that patients with AION often only were rescheduled for a follow up more than one week after initial onset of symptoms.

Hyperreflective dots, elsewhere referred as small dense particles (Framme et al., 2010) or hyperreflective foci (Framme et al., 2012), have been observed in several retinal diseases including age-related macular degeneration (AMD) (Framme et al., 2010) diabetic macular edema (DME) (Bolz et al., 2009; Ota et al., 2010; Horii et al., 2012) and retinal vein occlusion (RVO) (Coscas et al., 2011; Ogino et al., 2012) but their origin remains still controversial. According to one hypothesis hyperreflective dots may represent inflammatory cells or activated macrophages that phagocytose degenerated retinal neurons (Vujosevic et al., 2013; Framme et al., 2010; Nowak, 2006). Indeed, the presence of activated macrophages has been observed in various conditions of retinal disease (Sekiryu et al., 2012; Omri et al., 2011; Cruz-Guilloty et al., 2013).

However, the beneficial or deleterious role of macrophages in the course of AION, and in white matter stroke in general, is still controversial. Macrophages are a heterogeneous population of cells that can lead either to inflammation or act in an anti-inflammatory manner promoting angiogenesis. This heterogeneity brings limitations on the investigation of the role

of these cells in the pathophysiology of retinal disease. It has been previously suggested that macrophage invasion into the retina precedes degeneration and retinal cell death under pathological conditions (Caicedo et al., 2005). Thus, one could speculate that activation of resident microglia or recruitment of circulating macrophages is involved in triggering or facilitating retinal degeneration. Activated macrophages are believed to have a greater destructive potential compared to resident microglia (Gordon, 1995), therefore, invading macrophages may cause alterations in retinal function. Additional studies are necessary for the investigation of the role of these cells in the pathophysiology of AION. Such studies could provide useful information and may help to establish therapeutic targets for the treatment of AION.

5. CONCLUSIONS

The animal experiments of the present study suggested that the hyperreflective dots that are detected in the OCT scans correspond to activated macrophages invading the retina in the early phase of laser-induced model of optic neuropathy and may contribute to changes in the retinal physiology. The involvement of inflammatory components such as microglia/macrophages in CNS ischemia following stroke has been previously characterized (Kochanek and Hallenbeck, 1992). Thus, if hyperreflective dots correspond to activated macrophages, then SD-OCT could be used as a new method to monitor inflammatory components during anterior ischemic optic neuropathy.

6. ACKNOWLEDGMENTS

preparation of the manuscript. The authors are responsible for the content and writing of this paper.

Author contributions

DK. Conducting experiments, acquiring data, analyzing data, writing the manuscript

NH. Conducting experiments, acquiring data, analyzing data

AE. Performing experimental procedures and critical reviewing of the manuscript

MZ. Designing research studies, analyzing data, writing the manuscript, conducting experiments

REFERENCES:

AHMED, Z., SHAW, G., SHARMA, V. P., YANG, C., MCGOWAN, E. & DICKSON, D. W. 2007. Actin-binding proteins coronin-1a and IBA-1 are effective microglial markers for immunohistochemistry. *J Histochem Cytochem,* 55**,** 687-700.

BERNSTEIN, S. L., GUO, Y., KELMAN, S. E., FLOWER, R. W. & JOHNSON, M. A. 2003. Functional and cellular responses in a novel rodent model of anterior ischemic optic neuropathy. *Invest Ophthalmol Vis Sci,* 44**,** 4153-62.

BOLZ, M., SCHMIDT-ERFURTH, U., DEAK, G., MYLONAS, G., KRIECHBAUM, K., SCHOLDA, C. & DIABETIC RETINOPATHY RESEARCH GROUP, V. 2009. Optical coherence tomographic hyperreflective foci: a morphologic sign of lipid extravasation in diabetic macular edema. *Ophthalmology,* 116**,** 914-20.

CAICEDO, A., ESPINOSA-HEIDMANN, D. G., HAMASAKI, D., PINA, Y. & COUSINS, S. W. 2005. Photoreceptor synapses degenerate early in experimental choroidal neovascularization. *J Comp Neurol,* 483**,** 263-77.

CHUNG, S. M., GAY, C. A. & MCCRARY, J. A., 3RD 1994. Nonarteritic ischemic optic neuropathy. The impact of tobacco use. *Ophthalmology,* 101**,** 779-82.

COSCAS, G., LOEWENSTEIN, A., AUGUSTIN, A., BANDELLO, F., BATTAGLIA PARODI, M., LANZETTA, P., MONES, J., DE SMET, M., SOUBRANE, G. & STAURENGHI, G. 2011. Management of retinal vein occlusion--consensus document. *Ophthalmologica,* 226**,** 4-28.

CRUZ-GUILLOTY, F., SAEED, A. M., ECHEGARAY, J. J., DUFFORT, S., BALLMICK, A., TAN, Y., BETANCOURT, M., VITERI, E., RAMKHELLAWAN, G. C., EWALD, E., FEUER, W., HUANG, D., WEN, R., HONG, L., WANG, H., LAIRD, J. M., SENE, A., APTE, R. S., SALOMON, R. G., HOLLYFIELD, J. G. & PEREZ, V. L. 2013. Infiltration of proinflammatory m1 macrophages into the outer retina precedes damage in a mouse model of age-related macular degeneration. *Int J Inflam,* 2013**,** 503725.

DOUGLAS, S. D. & TULUC, F. 2012. Morphology of monocytes and macrophages. *In:* MARSHALL A. LICHTMAN, T. J. K., URI SELIGSOHN, KENNETH KAUSHANSKY, JOSEF T. PRCHAL (ed.) *Williams Hematology.* Eighth Edition ed. New York, NY: McGraw-Hill.

FRAMME, C., SCHWEIZER, P., IMESCH, M., WOLF, S. & WOLF-SCHNURRBUSCH, U. 2012. Behavior of SD-OCT-detected hyperreflective foci in the retina of anti-VEGF-treated patients with diabetic macular edema. *Invest Ophthalmol Vis Sci,* 53**,** 5814-8.

FRAMME, C., WOLF, S. & WOLF-SCHNURRBUSCH, U. 2010. Small dense particles in the retina observable by spectral-domain optical coherence tomography in age-related macular degeneration. *Invest Ophthalmol Vis Sci,* 51**,** 5965-9.

GARCIA-VALENZUELA, E. & SHARMA, S. C. 1999. Laminar restriction of retinal macrophagic response to optic nerve axotomy in the rat. *J Neurobiol,* 40**,** 55-66.

GOLDENBERG-COHEN, N., KRAMER, M., BAHAR, I., MONSELISE, Y. & WEINBERGER, D. 2004. Elevated plasma levels of interleukin 8 in patients with acute anterior ischaemic optic neuropathy. *Br J Ophthalmol,* 88**,** 1538-40.

GORDON, S. 1995. The macrophage. *Bioessays,* 17**,** 977-86.

GUYER, D. R., MILLER, N. R., AUER, C. L. & FINE, S. L. 1985. The risk of cerebrovascular and cardiovascular disease in patients with anterior ischemic optic neuropathy. *Arch Ophthalmol,* 103**,** 1136-42.

HAYREH, S. S. 1974. Anterior ischaemic optic neuropathy. I. Terminology and pathogenesis. *Br J Ophthalmol,* 58**,** 955-63.

HAYREH, S. S. 2014. Ocular vascular occlusive disorders: natural history of visual outcome. *Prog Retin Eye Res,* 41**,** 1-25.

HAYREH, S. S., JOOS, K. M., PODHAJSKY, P. A. & LONG, C. R. 1994. Systemic diseases associated with nonarteritic anterior ischemic optic neuropathy. *Am J Ophthalmol,* 118**,** 766-80.

HORII, T., MURAKAMI, T., NISHIJIMA, K., AKAGI, T., UJI, A., ARAKAWA, N., MURAOKA, Y. & YOSHIMURA, N. 2012. Relationship between fluorescein pooling and optical coherence tomographic reflectivity of cystoid spaces in diabetic macular edema. *Ophthalmology,* 119**,** 1047-55.

JUNG, S., ALIBERTI, J., GRAEMMEL, P., SUNSHINE, M. J., KREUTZBERG, G. W., SHER, A. & LITTMAN, D. R. 2000. Analysis of fractalkine receptor CX(3)CR1 function by targeted deletion and green fluorescent protein reporter gene insertion. *Mol Cell Biol,* 20**,** 4106-14.

KOCHANEK, P. M. & HALLENBECK, J. M. 1992. Polymorphonuclear leukocytes and monocytes/macrophages in the pathogenesis of cerebral ischemia and stroke. *Stroke,* 23**,** 1367-79.

LANGMANN, T. 2007. Microglia activation in retinal degeneration. *J Leukoc Biol,* 81**,** 1345-51.

LEE, M. S., GROSSMAN, D., ARNOLD, A. C. & SLOAN, F. A. 2011. Incidence of nonarteritic anterior ischemic optic neuropathy: increased risk among diabetic patients. *Ophthalmology,* 118**,** 959-63.

LEVIN, L. A. & LOUHAB, A. 1996. Apoptosis of retinal ganglion cells in anterior ischemic optic neuropathy. *Arch Ophthalmol,* 114**,** 488-91.

LOW, P. C., MANZANERO, S., MOHANNAK, N., NARAYANA, V. K., NGUYEN, T. H., KVASKOFF, D., BRENNAN, F. H., RUITENBERG, M. J., GELDERBLOM, M., MAGNUS, T., KIM, H. A., BROUGHTON, B. R., SOBEY, C. G., VANHAESEBROECK, B., STOW, J. L., ARUMUGAM, T. V. & MEUNIER, F. A. 2014. PI3Kdelta inhibition reduces TNF secretion and neuroinflammation in a mouse cerebral stroke model. *Nat Commun,* 5**,** 3450.

NOWAK, J. Z. 2006. Age-related macular degeneration (AMD): pathogenesis and therapy. *Pharmacol Rep,* 58**,** 353-63.

OGINO, K., MURAKAMI, T., TSUJIKAWA, A., MIYAMOTO, K., SAKAMOTO, A., OTA, M. & YOSHIMURA, N. 2012. Characteristics of optical coherence tomographic hyperreflective foci in retinal vein occlusion. *Retina,* 32**,** 77-85.

OMRI, S., BEHAR-COHEN, F., DE KOZAK, Y., SENNLAUB, F., VERISSIMO, L. M., JONET, L., SAVOLDELLI, M., OMRI, B. & CRISANTI, P. 2011. Microglia/macrophages migrate through retinal epithelium barrier by a transcellular route in diabetic retinopathy: role of PKCzeta in the Goto Kakizaki rat model. *Am J Pathol,* 179**,** 942-53.

OTA, M., NISHIJIMA, K., SAKAMOTO, A., MURAKAMI, T., TAKAYAMA, K., HORII, T. & YOSHIMURA, N. 2010. Optical coherence tomographic evaluation of foveal hard exudates in patients with diabetic maculopathy accompanying macular detachment. *Ophthalmology,* 117**,** 1996-2002.

SAITO, M., BARBAZETTO, I. A. & SPAIDE, R. F. 2013. Intravitreal cellular infiltrate imaged as punctate spots by spectral-domain optical coherence tomography in eyes with posterior segment inflammatory disease. *Retina,* 33**,** 559-65.

SALGADO, C., VILSON, F., MILLER, N. R. & BERNSTEIN, S. L. 2011. Cellular inflammation in nonarteritic anterior ischemic optic neuropathy and its primate model. *Arch Ophthalmol,* 129**,** 1583-91.

SALOMON, O., HUNA-BARON, R., KURTZ, S., STEINBERG, D. M., MOISSEIEV, J., ROSENBERG, N., YASSUR, I., VIDNE, O., ZIVELIN, A., GITEL, S., DAVIDSON, J., RAVID, B. & SELIGSOHN, U. 1999. Analysis of prothrombotic and vascular risk factors in patients with nonarteritic anterior ischemic optic neuropathy. *Ophthalmology,* 106**,** 739-42.

SEKIRYU, T., IIDA, T., SAKAI, E., MARUKO, I., OJIMA, A. & SUGANO, Y. 2012. Fundus autofluorescence and optical coherence tomography findings in branch retinal vein occlusion. *J Ophthalmol,* 2012**,** 638064.

SLATER, B. J., VILSON, F. L., GUO, Y., WEINREICH, D., HWANG, S. & BERNSTEIN, S. L. 2013. Optic nerve inflammation and demyelination in a rodent model of nonarteritic anterior ischemic optic neuropathy. *Invest Ophthalmol Vis Sci,* 54**,** 7952-61.

THANOS, S. 1992. Sick photoreceptors attract activated microglia from the ganglion cell layer: a model to study the inflammatory cascades in rats with inherited retinal dystrophy. *Brain Res,* 588**,** 21-8.

VAZ-PEREIRA, S., ZARRANZ-VENTURA, J., SIM, D. A., KEANE, P. A., SMITH, R., EGAN, C. A. & TUFAIL, A. 2015. Optical Coherence Tomography Features of Active and Inactive Retinal Neovascularization in Proliferative Diabetic Retinopathy. *Retina*.

VUJOSEVIC, S., BINI, S., MIDENA, G., BERTON, M., PILOTTO, E. & MIDENA, E. 2013. Hyperreflective intraretinal spots in diabetics without and with nonproliferative diabetic retinopathy: an in vivo study using spectral domain OCT. *J Diabetes Res,* 2013**,** 491835.

WILMS, H., HARTMANN, D. & SIEVERS, J. 1997. Ramification of microglia, monocytes and macrophages in vitro: influences of various epithelial and mesenchymal cells and their conditioned media. *Cell Tissue Res,* 287**,** 447-58.

ZHANG, C., GUO, Y., MILLER, N. R. & BERNSTEIN, S. L. 2009. Optic nerve infarction and post-ischemic inflammation in the rodent model of anterior ischemic optic neuropathy (rAION). *Brain Res,* 1264**,** 67-75.

ZHANG, C. & TSO, M. O. 2003. Characterization of activated retinal microglia following optic axotomy. *J Neurosci Res,* 73**,** 840-5.

Figure Legends

Figure 1: Retinal morphology and retinal microglia in experimental laser-induced optic neuropathy (eLiON). A, B. Representative retinal OCT scans of the optic nerve before (A, n=10) and 3 days after eLiON (B, n=10). The scan location is indicated in the infrared fundus photographs (left). Hyperreflective dots (representative cell enlarged in yellow box) are observed 3 days after eLiON in the vitreous next to the swollen optic disc. **C-E.** Representative images of hematoxylin-eosin staining in control bone marrow chimera mice (C, n=4) and eLiON-subjected bone marrow chimera mice (D, n=6). In eLiON (D) cells are found in the vitreous and close to the optic nerve head (E) 7 days after the laser application. Retinal folds are present in the peripapillary area (arrows). Asterisk is optic nerve head. **F-J**. Co-localization studies in bone marrow chimera mice reveal infiltration of grafted GFP-positive cells into the retina of eLiON mice (I, n=6). All GFP-positive cells express the microglial marker Iba-1 in eLiON and have amoeboid morphology (H, Iba-1; I, GFP; J, merged). GFP-positive cells are absent in control retina (F, n=4), where Iba-1-positive cells are less abundant and have a ramified morphology (G). Scale bars in OCT scans in A: 200 μm; in C, D, F, H, I, J: 200 μm; in E, G: 20 μm. Magnification in C, D, F, H, I, J: 10x; in E: 100x; in G: 40x.

Figure 2: Comparison of experimental laser-induced optic neuropathy (eLiON) in mice and anterior ischemic optic neuropathy (AION) in humans. A. Mouse retinal thickness around the optic nerve head before and after eLiON (n=9, ***$p<0.001$ compared to Baseline, two way ANOVA). **B.** Representative transverse optical coherence tomography scan of the optic nerve head (top scans, location shown on respective near-infrared fundus image) and retinal nerve fibre layer thickness scan (bottom scans) in mice 3 days post eLiON. **C.**
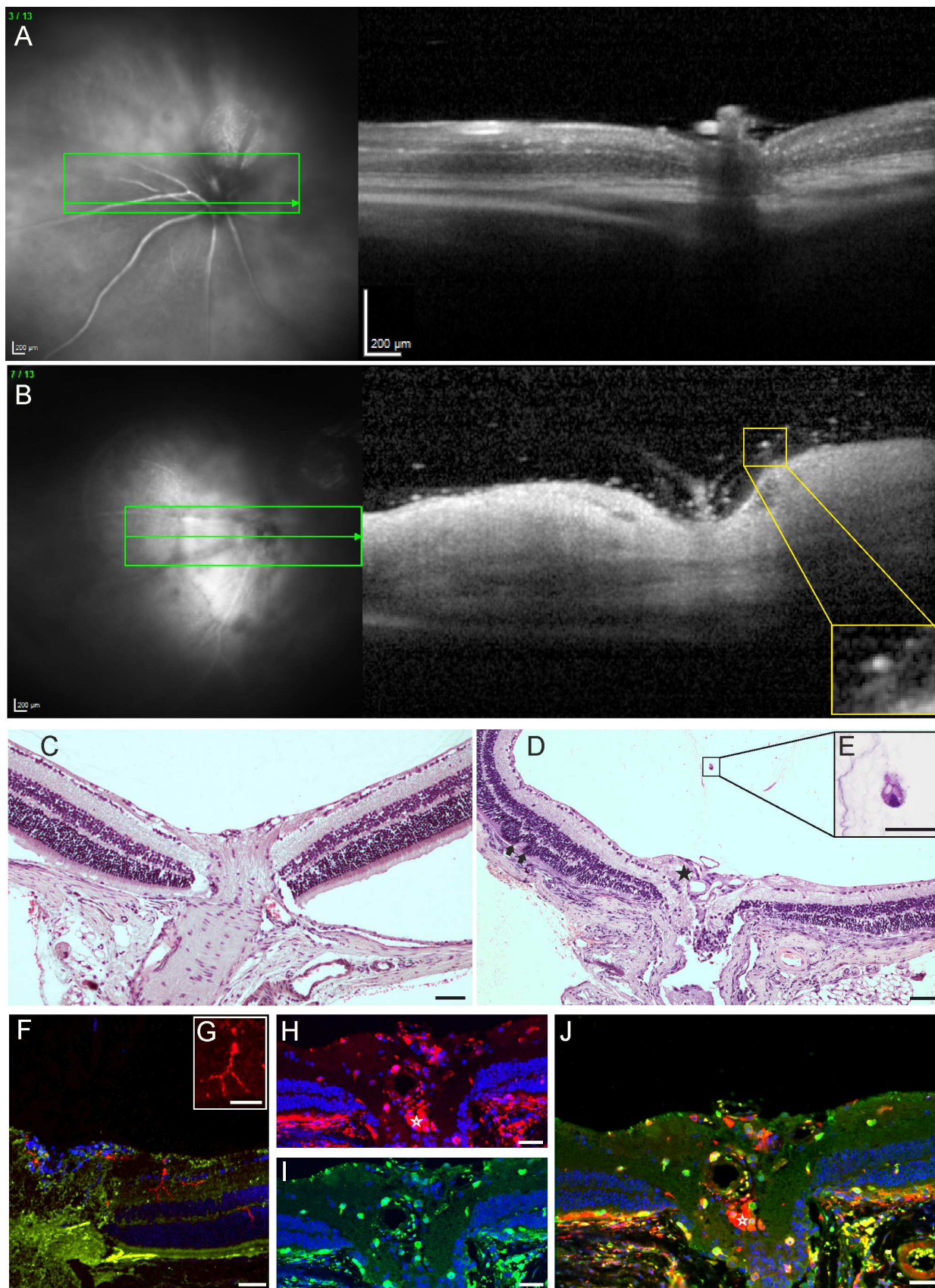
Macrophage dynamics with representative FACS plots (left panel) and bar graphs of macrophage accumulation in the retina at indicated days after eLiON (n≥6, **p<0.01, ***p<0.001 compared to CTRL, one way ANOVA, data from one of at least 2 independent experiments are shown) demonstrating macrophage cell population (top right quarter, $CD45^+F4/80^+CD11b^+$) in control (CTRL) and eLiON retinas at days 3, 7 and 14 after the laser application. **D.** Study design and patient selection **E.** Representative transverse optical coherence tomography scan of the optic nerve head (top scans, location shown on respective near-infrared fundus image) and retinal nerve fibre layer thickness scan (bottom scans) of a human patient 1 week after initial symptoms. Hyperreflective dots are apparent in the human retina and adjacent vitreous (yellow squares). **F.** Quantification of hyperreflective dots in vitreous (top) and retina (bottom) (vitreous: 1 week, n=11; 2 weeks, n=13; 3-4 weeks, n=7; 5-7 weeks, n=5; 8-14 weeks, n=5; 15-70 weeks, n=12; retina: 1 week, n=11; 2 weeks, n=11; 3-4 weeks, n=6; 5-7 weeks, n=5; 8-14 weeks, n=5; 15-70 weeks, n=10). A significant increase of hyperreflective dots was observed in the retina (p<0.01, ordinary one way ANOVA). Highest levels were detected two weeks after initial symptoms and were statistically different from the counts 15-70 days weeks after initial symptoms (**p<0.01).
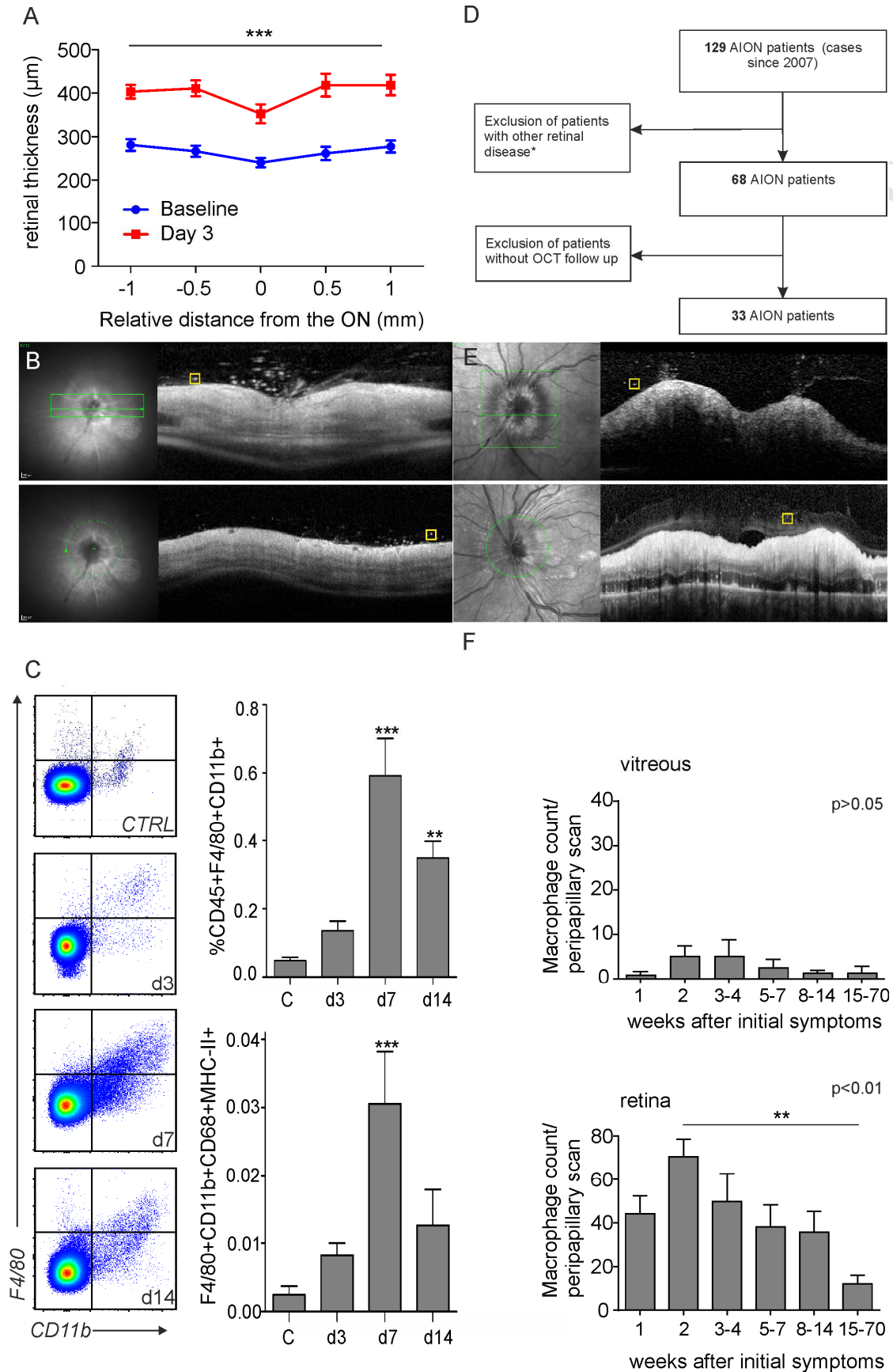
Figure 3: Kinetics of peripapillary hyperreflective dots in different retinal layers in humans with anterior ischemic optic neuropathy. Serial optical coherence tomography scans of a representative patient at 1, 2, 3-4 and 15-70 weeks after onset of symptoms (left panel, **A, B, C** and **D,** respectively). **E.** Serial counts in different retinal layers. A significant change of hyperreflective dots density over time was detected only in the outer plexiform (p<0.01, ordinary one way ANOVA) and the outer nuclear retinal layer (p<0.05, ordinary one way ANOVA) (1 week, n=10; 2 weeks, n=11; 3-4 weeks, n=5; 5-7 weeks, n=6; 8-14 weeks, n=4; 15-70 weeks, n=4). No statistical significant changes were observed in the ganglion cell layer, inner plexiform or inner nuclear layer (p>0.05, ordinary one way ANOVA).

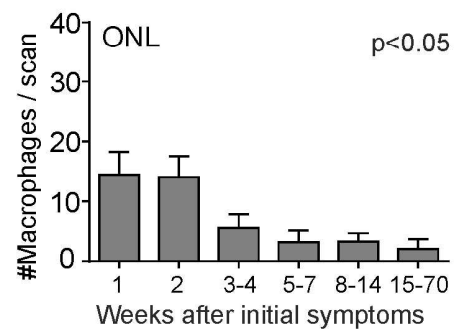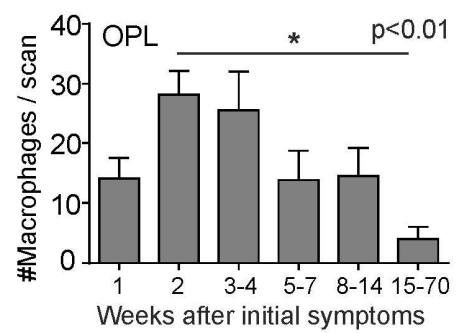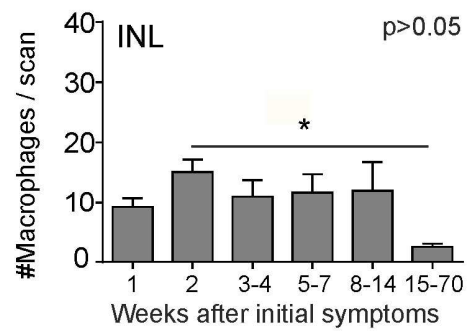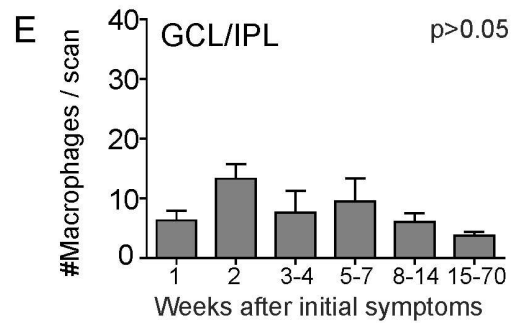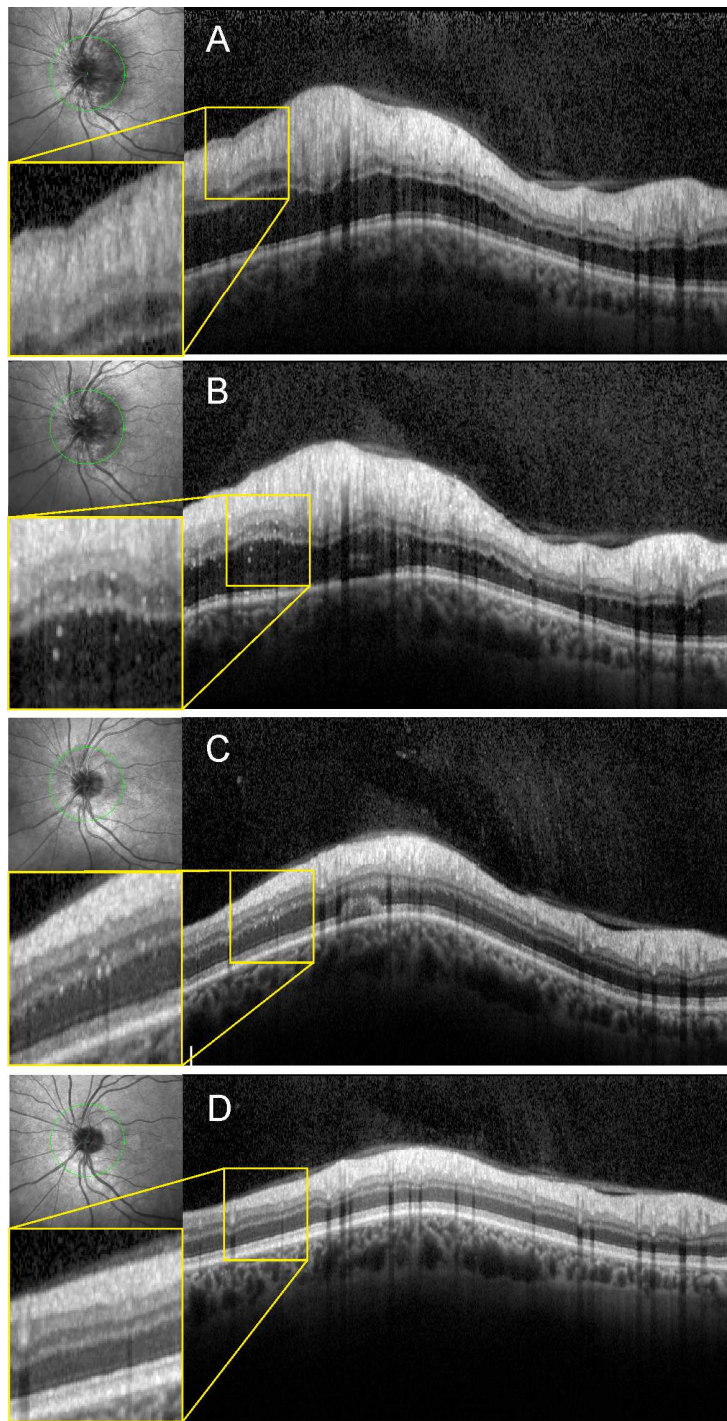Statistically significant differences were observed between different time points in the INL and the OPL (INL: week 2 vs week 15-70, $*p<0.05$; OPL: week 2 vs week 15-70, $*p<0.05$; ordinary One way ANOVA followed by Tukey`s post-hoc analysis). GCL, ganglion cell layer; IPL, inner plexiform layer; INL, inner nuclear layer; OPL, outer plexiform layer; ONL, outer nuclear layer.

Table 1: Demographic data

	A-AION	NA-AION	total
n	10	23	33
age	77 ± 6.9	67 ± 13	72 ± 12
Gender (male:female)	4:6	13:10	17:16
Diabetes	1	4	5
Arterial hypertension	2	7	9
Biopsy	10	3	13
Eye (OD:OS)	4:6	16:9	20:15
Visual acuity at presentation (LogMAR)	2.16	1.04	2.65

A

retinal thickness (µm) vs Relative distance from the ON (mm)
***
Baseline
Day 3

D

129 AION patients (cases since 2007)

Exclusion of patients with other retinal disease*

68 AION patients

Exclusion of patients without OCT follow up

33 AION patients

B

E

C

CTRL
d3
d7
d14

F4/80
CD11b

%CD45+F4/80+CD11b+
C   d3   d7   d14
***
**

F4/80+CD11b+CD68+MHC-II+
C   d3   d7   d14
***

F

vitreous
p>0.05
Macrophage count/peripapillary scan
weeks after initial symptoms
1   2   3-4   5-7   8-14   15-70

retina
p<0.01
**
Macrophage count/peripapillary scan
weeks after initial symptoms
1   2   3-4   5-7   8-14   15-70

Highlights

- Macrophages are recruited via the optic nerve into the surrounding retina after experimental anterior ischemic optic neuropathy
- Hyperreflective dots in spectral domain optical coherence tomography correspond to activated macrophages
- Macrophage accumulation can be imaged and quantified *in vivo* with SD-OCT
- Spectral domain optical coherence tomography could be used to assess the inflammatory components during optic nerve ischemia